



Original software publication

1DCSEMQWE: 1D Controlled Source Electromagnetic Method in Geophysics Using Quadrature With Extrapolation

Pham Ngoc Kien ^{a,b}, Sang-Mook Lee ^{a,*}^a School of Earth and Environmental Sciences, Seoul National University, 08826, Republic of Korea^b Faculty of Oil and Gas, Hanoi University of Mining and Geology, Hanoi, 100000, Viet Nam

ARTICLE INFO

Article history:

Received 9 April 2022

Received in revised form 22 May 2022

Accepted 15 June 2022

Keywords:

Numerical solution

Electromagnetics

One-dimensional

Arbitrarily oriented dipole

Integral equation

ABSTRACT

We present a C++ package entitled 1D Controlled Source Electromagnetic Method using Quadrature With Extrapolation (1DCSEMQWE), which computes the electromagnetic field for a one-dimensional model in geophysics. This package supports the computation for both electric and magnetic dipole sources. Transmitters and receivers can be placed anywhere in the layered model. The formulation of the electromagnetic field in the frequency domain avoids using positive exponential terms, leading to higher accuracy. In particular, we introduce a new computation tool using quadrature with extrapolation for integral evaluation. Our tool addresses the numerical error occurring in the previous quadrature rule algorithm and gives users the ability to control the precision of the computed electromagnetic field.

© 2022 The Author(s). Published by Elsevier B.V. This is an open access article under the CC BY license (<http://creativecommons.org/licenses/by/4.0/>).

Code metadata

Current code version

Permanent link to code/repository used for this code version

Permanent link to reproducible capsule

Legal code license

Code versioning system used

Software code languages, tools, and services used

Compilation requirements, operating environments, and dependencies

If available, link to developer documentation/manual

Support email for questions

v1

<https://github.com/ElsevierSoftwareX/SOFTX-D-22-00086>

GNU General Public License (GPL) v3

none

C++

g++; Unix, Linux; Boost

<https://github.com/phamngockien/1DCSEMQWE/blob/main/doc/Manual.pdf>phamngockien@snu.ac.kr

1. Motivation and significance

The geophysical electromagnetic method usually considers the quasi-static approximation of Maxwell's equations where the displacement current can be neglected at low frequencies. Because the electromagnetic (EM) field is sensitive to the change in the resistivity of subsurface geological settings, this method has various applications, such as hydrocarbon exploration [1], reservoir monitoring [2], and geological studies [3].

One-dimensional (1D) simulation is an important step in the controlled source electromagnetic method. The physical behavior of the method can be examined by using the electromagnetic

(EM) field derived from the 1D simulation [4]. In terms of applications, the 1D simulation is often used to validate the accuracy of the higher dimensional computation [5], design practical measurement [6], and quick data interpretation [3]. In particular, several two- and three-dimensional algorithms utilize the solution of the 1D problem as the background field, which helps to reduce the mesh size and the singularity near the position of the transmitter [7,8].

We propose a C++ software package named 1D Controlled Source Electromagnetic Method using Quadrature With Extrapolation (1DCSEMQWE). Our program supports an accurate numerical computation of the EM field in a 1D model where the transmitter and receiver can be placed anywhere. The computations for arbitrarily oriented electric and magnetic dipole sources are also included. We provide an input file where users can

* Corresponding author.

E-mail address: smlee@snu.ac.kr (Sang-Mook Lee).

change the model settings, transmitter–receiver geometry, and the desired precision of the EM field. The model parameters and the EM field for further analysis are then produced in comma-separated values (CSV) files.

Our software computes the EM field based on the vector potential technique. The electric and magnetic fields in any layer (i th) of a 1D model are expressed as the superposition of those in TM and TE mode as

$$\begin{cases} E_i = E_i^{TM} + E_i^{TE}, \\ H_i = H_i^{TM} + H_i^{TE}, \end{cases} \quad (1)$$

in which

$$\begin{cases} E_i^{TE} = -\nabla \times F_i^{TE}, \\ H_i^{TE} = -\sigma_i F_i^{TE} + \frac{1}{i\omega\mu} \nabla \nabla \cdot F_i^{TE}, \\ E_i^{TM} = -i\omega\mu A_i^{TM} + \frac{1}{\sigma_i} \nabla \nabla \cdot A_i^{TM}, \\ H_i^{TM} = \nabla \times A_i^{TM}. \end{cases} \quad (3)$$

Here, i is the imaginary unit, $\omega = 2\pi f$ is the angular frequency (rad/s), μ is the magnetic permeability (H/m), and σ is the electrical conductivity (S/m). The subscript $(\cdot)_i$ denotes the index of the receiver layer. A^{TM} and F^{TE} represent the vector potentials in TM and TE mode, respectively.

In literature, this technique is adopted in several algorithms. For instance, the algorithms in [9–11] express the vector potential as

$$A_i^{TM} = \frac{1}{4\pi} \int_{-\infty}^{\infty} \int_{-\infty}^{\infty} [a_i e^{u_i(z-z_s)} + b_i e^{-u_i(z-z_s)}] e^{i(k_x x + k_y y)} dk_x dk_y, \quad (4)$$

$$F_i^{TE} = \frac{1}{4\pi} \int_{-\infty}^{\infty} \int_{-\infty}^{\infty} [c_i e^{u_i(z-z_s)} + d_i e^{-u_i(z-z_s)}] e^{i(k_x x + k_y y)} dk_x dk_y, \quad (5)$$

where a_i , b_i , c_i , and d_i are the potential coefficients; z and z_s are the vertical positions of the receiver and the transmitter, respectively; k_x and k_y are the spatial wavenumbers in x - and y -directions;

$$u_i^2 = k_x^2 + k_y^2 + i\omega\mu\sigma_i. \quad (6)$$

This expression involves the computation of a positive exponential term. When the vertical distance between the transmitter and receiver is large, the positive exponential usually leads to numerical instability [12]. Another algorithm [13] addresses this numerical problem for the electric dipole source by reformulating the equation without any positive exponential term. This paper extends the formulation in [13] for arbitrary dipole types. Our detailed recursive formulation of the vector potential is described in [Appendix](#).

The formulation of the EM field ends up with an integral equation, where the EM field is derived by taking the derivative of the vector potential as

$$F(x, y, z) = \int_0^{\infty} f_0(\lambda) J_0(\lambda\rho) d\lambda + \int_0^{\infty} f_1(\lambda) J_1(\lambda\rho) d\lambda, \quad (7)$$

where $\lambda^2 = k_x^2 + k_y^2$; J_0 and J_1 are the Bessel functions of orders 0 and 1, respectively; and F represents either the electric or the magnetic field. Function $f_0(\lambda)$ is derived when there is no derivative with respect to x and y ; otherwise, function $f_1(\lambda)$ is involved. The integrals in Eq. (7) are often evaluated by the digital

filter method [14,15]. An alternative is to use the quadrature-with-extrapolation technique (QWE) [16], in which the infinite integrals by summing over a finite number of partial intervals as

$$F = \sum_{i=0}^n F_i \quad (8)$$

$$\text{with } F_i = \int_{k_i}^{k_{i+1}} f_0(k) J_0(k\rho) dk + \int_{k_i}^{k_{i+1}} f_1(k) J_1(k\rho) dk. \quad (9)$$

The quadrature rule is used to calculate each partial integral F_i . An extrapolation loop is then carried out until the extrapolated sum of F_i converges [17]. The criterion of the convergence is

$$|S_i - S_{i-1}| \leq \varepsilon_r S_i + \varepsilon_a, \quad (10)$$

where ε_r and ε_a are the relative and absolute tolerances, respectively; S_i is the extrapolated result at the i th iteration.

The previous QWE computation [16,18] produces an error when the vertical transmitter–receiver distance is large. Therefore, we modify the previous QWE technique to ensure the accuracy of the EM field. Our modification is described in [Fig. 1](#).

There exist several software for 1D EM simulation, such as Dipole1D [13], emmod [19], empymod [18], and MatlabCSEM1D [11]. The Dipole1D only deals with the electric dipole source; the MatlabCSEM1D may produce an unstable EM field due to the positive exponential in the formulation. The empymod, based on the emmod, supports the computation for both electric and magnetic dipole sources inside a layered earth model based on the digital filter method. In terms of programming language, the empymod is implemented in python. Although C++ has an advantage over python in high-performance computation, it is rarely used in the geophysical community. In this paper, we manage to develop our package in C++. Our program is the first open-source package that solves the 1D EM problem with all dipole types for arbitrary transmitter–receiver configuration by the QWE technique under the GNU license [20]. In the future, the QWE function of our program can be combined with the previous software for 1D analysis. The creation of 1DCSEMQWE also aims at coupling with available open-source libraries, such as Deal.II [21], Fenics [22], and PETSc [23], for two- and three-dimensional EM simulations.

2. Software description

2.1. Software architecture

1DCSEMQWE utilizes Boost library [24] for Bessel function evaluation and the Gauss quadrature code from Deal.II library [21]. We also provide several examples in Python [25] with the use of Numpy [26], Matplotlib [27], and Pandas [28] libraries for efficiency. These examples demonstrate how to generate an input file and produce the data analysis.

[Fig. 2](#) is the computation procedure of our program. The geometrical and physical parameters are included in an input file. The program loads the file and then precomputes some variables including quadrature points, the product of the Bessel function and weight at those points, and the thickness of each layer before calculating the EM fields at each receiver. This way of computation reduces the time cost of the program because those variables are reusable for all transmitters and frequencies. The 1D forward problem for each transmitter and frequency is solved in the next step. Finally, the output block saves the EM responses for the transmitter–receiver configuration in separate files concerning the frequencies used in the computation.

a. Previous QWE [16]	b. Our modification
<pre> Compute the first partial integral F0 (a delay term) # Extrapolation loop For i = 1 to n S(i) = S(i-1) + Fi aux2 = 0 # Recursive loop For k = i downto 1 aux1 = aux2 aux2 = S(k-1) dddf = S(k) - aux2 if dddf < smallest positive floating point number S(k-1) = largest floating point number else S(k-1) = aux1 + 1/ddff # Compute this extrapolation E(i-1) = S[mod(i,2)] + F0 # Convergence check if i > 1 check for convergence If the condition is matched then exit the extrapolation loop, else compute the next iteration of i. # Get the result of extrapolation Extrapolation result = E(i-1) at the latest iteration of i. Set the Extrapolation result, which is equal to the largest floating point number, to zero. </pre>	<pre> # Extrapolation loop For i = 0 to n if i = 0 then S(i) = Fi E(i) = S(i) else S(i) = S(i-1) + Fi aux2 = 0 # Recursive loop For k = i downto 1 aux1 = aux2 aux2 = S(k-1) dddf = S(k) - aux2 if dddf < smallest positive floating point number S(k-1) = largest floating point number else S(k-1) = aux1 + 1/ddff # Compute this extrapolation E(i) = S[mod(i,2)] # Convergence check if i > 0 check for convergence If the condition is matched then exit the extrapolation loop, else compute the next iteration of i. # Get the result of extrapolation Extrapolation result = E(i) at the latest iteration of i. </pre>

Fig. 1. Modification of the implementation of the QWE technique. (size: 120 mm × 85 mm).

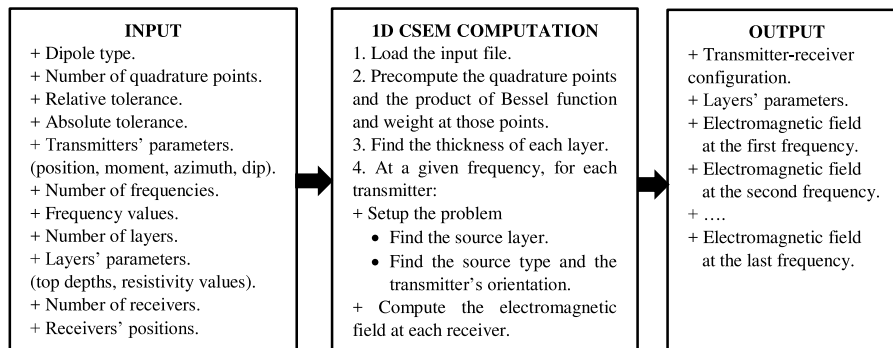


Fig. 2. The flow chart of our program. (size: 130 mm × 49 mm).

2.2. Software functionalities

1DCSEMQWE currently supports numerical computation in the SI units with the Cartesian coordinate system. It computes all components of the electromagnetic field in x-, y-, and z-directions for both electric and magnetic dipole sources. The model consists of many layers with isotropic resistivity, in which the transmitter can be arbitrarily oriented. Also, the computations for various frequencies are carried out simultaneously for a given transmitter–receiver configuration.

The functionalities of the 1DCSEMQWE can be subdivided into its five main classes. The Prms class stores all the input parameters and precomputes the quadrature points, weights, and Bessel functions which are required by the QWE computation. The QGauss class implements the Gauss quadrature rule which is called by the Prms class for the precomputation. The GET_CSEM1D_FD_QWE class produces the EM fields at the receivers' location for a given transmitter at a certain frequency value. It first sets up the equations for each transmitter at each frequency and then derives the EM fields by evaluating the integral equation using the QWE technique (see also step 4 of the solver block in Fig. 2). The output_1D_CSEM_solution class saves the EM fields computed into an output file. The Run1DCSEM class carries out the computation procedure shown in Fig. 2 by calling the functions in the other classes.

3. Illustrative examples

We provide an illustrative example using the canonical model [29]. This model consists of five horizontal layers. The upper-most layer is an air medium with the resistivity of 10^{12} Ohmmeter underlain by seawater of 0.3 Ohmmeter. Below the seafloor is a resistive reservoir of 100 Ohmmeter embedded within a more conductive seafloor layer of 1 Ohmmeter. The layer interfaces are located at $z = 0, 1000, 2000,$ and 2100 m. The model has been investigated in the literature for 1D synthetic data analysis [13] and validation of three-dimensional CSEM simulation [30].

Fig. 3 summarizes the parameters required in the input file with the comments on how to build the canonical model and the transmitter–receiver configuration. Users are free to choose the source type, the position and orientation of the transmitter, the receiver position, and the frequencies at which the measurement is obtained. In particular, the number of quadrature points and the tolerances for the numerical computation of the integral are easily set for precision control. This example used 101 quadrature points and small tolerances to compute the “truth” electromagnetic field [16].

Our program can compute the field at different frequencies for a given transmitter–receiver configuration. Fig. 4 illustrates the amplitude (left panels) and phase (right panels) of the electromagnetic (EM) field produced from the input file in Fig. 3. The

```

# DIPOLE TYPE: 0 ! Types: 0 for electric dipole source, 1 for magnetic dipole source.
# NQUAD: 101 ! Number of quadrature points to evaluate the integral.
# RTOL: 1e-12 ! Relative tolerance for convergence criteria of the QWE technique.
# ATOL: 1e-30 ! Absolute tolerance for convergence criteria of the QWE technique.
! This section lists the number of transmitters and then their parameters.
! The azimuth ranges from [0, 360] with a value of 0 in x-direction
! and has positive value w.r.t counter clockwise direction.
! The dip ranges from [-90, 90] degrees where -90 is upward direction and vise versa.
! X Y Z Moment Azimuth Dip
# TRANSMITTERS: 11
0 0 950 1 90 0
0 1000 950 1 90 0
0 2000 950 1 90 0
0 3000 950 1 90 0
0 4000 950 1 90 0
0 5000 950 1 90 0
0 6000 950 1 90 0
0 7000 950 1 90 0
0 8000 950 1 90 0
0 9000 950 1 90 0
0 10000 950 1 90 0
! This section lists the number of frequencies, and then their values.
# FREQUENCIES: 2
0.25
1.0
! This section gives the number of layers, their top depths, and resistivities (Ohmm).
# LAYERS: 5
-100000 1e12
0 .30
1000 1.0
2000 100
2100 1.0
! This section lists the number of receivers, and then their positions in x, y, z coordinates.
# RECEIVERS: 1
0 0 1000

```

Fig. 3. An illustrative example of an input file to compute the electromagnetic field of the canonical model. (size: 90 mm × 115 mm).

range is the horizontal offset between the transmitter and the receiver. In Fig. 4, there was a typical decrease in the amplitude versus offset of the field. The phase of the EM field changed differently with two frequencies. In particular, the amplitude of both electric and magnetic fields at a frequency of 1 Hz decayed more rapidly than those at 0.25 Hz. The reason is that the negative exponential term is smaller at a higher frequency, leading to a faster decay of the EM field.

We validated the improvement of our modified QWE technique by comparing the EM field computed by 1DCSEMQWE with the analytic solution [12] and the field produced by the previous QWE [16]. In this example, we examined a full space, homogeneous medium with a resistivity of 1 Ohmmeter. An x-oriented electric dipole source was located at the origin. Receivers were located at $x = 300$ meter, $y = 0$ meter, and $z = 0$ to 3000 meter. Fig. 5 illustrates that the field computed by our technique was well-agreed with the analytic solution, whereas the previous QWE technique failed to compute the field at depths between 1500 and 3000 m. Our modification converged rapidly at the first extrapolation iteration to the exact solution at large vertical distances between transmitter and receivers. In contrast, the previous technique produced zero at three iterations (see Fig. 1).

Our final example demonstrates the ability of 1DCSEMQWE for computing the EM field anywhere within a three-dimensional (3D) domain. Here, the canonical was used again with a z-oriented magnetic dipole source. The source was located in the reservoir layer, at $x = 0$ meter, $y = 0$ meter, and $z = 2050$ m. The EM field was computed within a mesh that ranged between -3000 and 3000 meters in x-, y-, and z-directions. The receiver spacing was 500 m. Fig. 6 showed the real-component vectors of the magnetic flux density (left) and the electric field (right) at the receivers' positions. The horizontal solid lines in Fig. 6c represent the interfaces between two adjacent layers. In a vertical cross-section (Fig. 6c), the magnetic flux density behaved differently in each layer due to the sensitivity of the EM field to resistivity. Since the vertical magnetic dipole source only produced the field in TE mode, the electric field in a horizontal section (Fig. 6d)

was parallel to the interfaces and perpendicular to the magnetic field (see also Fig. 6c). This behavior of the electric field is due to Faraday's law. The result in this example proved that our package could compute the EM field in the subsurface and the air layer.

4. Impact

The applicability for both electric and magnetic dipole sources is a major functionality of 1DCSEMQWE. In literature, various research has been carried out on the electric dipole for hydrocarbon exploration, predrill appraisal, and reservoir monitoring [2,4,29]. The typical concept of marine CSEM is to deploy the receivers on the seafloor to obtain the electromagnetic signal emitted by a deep-towing electric transmitter [1]. On the other hand, a crosswell configuration, where both transmitter and receiver are located inside boreholes, has proved important in reservoir characterization and fluid monitoring [31,32]. For the latter configuration, it is more convenient to use the magnetic dipole source. 1DCSEMQWE also supports the computation of EM field for arbitrarily oriented dipole; hence, it facilitates the practical survey where directional drilling technology is often used [33]. Furthermore, since the field computed by the integral equation is considered a semi-analytic solution, our program can be used to verify the result of other programs using the finite volume method [34].

Another important application of 1DCSEMQWE is to validate the 1D CSEM computation using the digital filter technique [16] and higher-dimensional numerical simulations [5]. The improvement of our modified QWE algorithm (Fig. 5) ensures the accuracy of the EM field for validation. Also, the ability to produce the field everywhere in the computation domain (Fig. 6) allows us to use the output of 1DCSEMQWE as a background response in higher dimensional simulations [7] by using other open-source libraries [21–23].

Our experiments presented in this paper are fundamental for other research fields such as magnetotelluric modeling [35] and the airborne EM method [7]. For instance, airborne systems usually use a dipole source because the size of the transmitters is small. Also, many interpretation procedures for the airborne EM method are based on 1D electromagnetic simulation [36].

Our program also has pedagogical value. It creates a simple interaction for the user to change all necessary parameters within a readable input file. Users can easily modify the parameters related to the QWE computation for investigating the numerical error of different numbers of quadrature points and different tolerances. Figs. 4 and 6 are intuitive examples that help to understand the behavior of the EM field for electric and magnetic dipole sources, respectively.

5. Conclusions

We have proposed a new computation tool for one-dimensional controlled-source electromagnetic (EM) simulation in the frequency domain using the quadrature-with-extrapolation (QWE) technique. Our tool addressed the numerical error of the previous QWE computation. Furthermore, we introduced a new formulation of the EM field based on the vector potential technique for all dipole types such that the instability due to the positive exponential term was avoided. Our algorithm was validated with the analytic solution in a homogeneous medium. Several fundamental experiments were also presented.

Our new algorithm has also been used to develop an open-source package in C++ that produces the electromagnetic field everywhere. Our package gives an ability to control the accuracy of the EM field by setting the number of quadrature points and the relative and absolute tolerances. It provides easy interaction

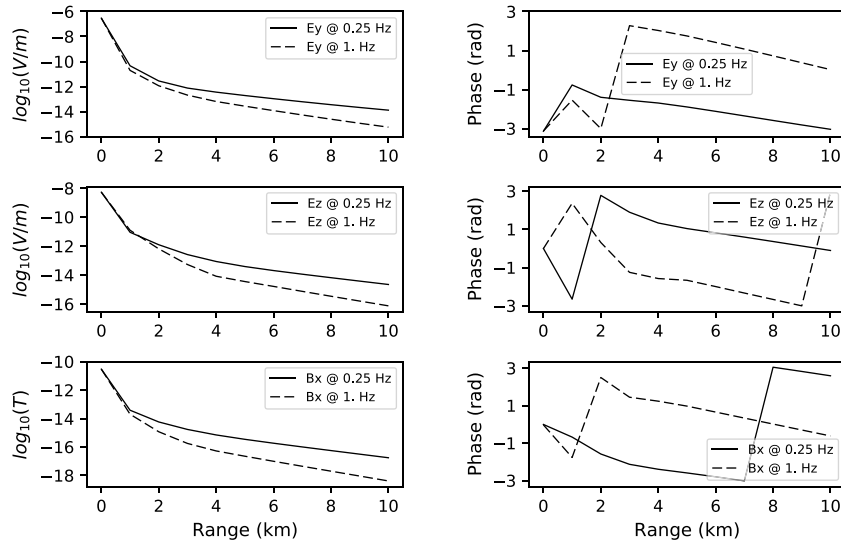


Fig. 4. Example of the electromagnetic field at 0.25 Hz (solid line) and 1 Hz (dashed line) computed from the input file in Fig. 3. (size: 120 mm \times 78 mm, 1000 dpi).

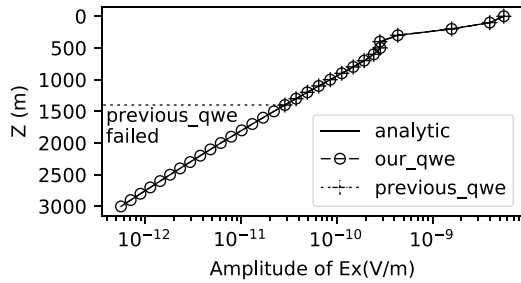


Fig. 5. Improvement of our modified QWE computation over the previous attempt. (size: 90 mm \times 44 mm, 1000 dpi).

through a readable input file without coding. Because of the fundamental nature of our algorithm, this new package has various applications and may reach large potential uses.

We will continue the development of this public package by fixing the bug, including other functionalities, and fulfilling the documentation. We highly appreciate contributions from other colleagues to our software in the future.

Declaration of competing interest

The authors declare that they have no known competing financial interests or personal relationships that could have appeared to influence the work reported in this paper.

Acknowledgments

Funds for this work were provided by the Korea Institute of Energy Technology Evaluation and Planning (KETEP) and the Ministry of Trade, Industry & Energy (MOTIE) of the Republic of Korea (No. 20168510030830 and 20194010000280).

We highly appreciate the insightful comments and suggestions from three reviewers, which significantly helps to improve the quality of our paper.

Appendix. Recursive formulation of EM field

We follow the work of [12] to formulate the equation for both electric and magnetic dipole sources, but a different definition

of the vector potential is used to avoid the positive exponential term. The formulae of the vector potentials for different dipole sources are given as follows.

x-oriented electric dipole source

We write the equations for the vector potentials in the i th layer as

$$A_i^{TM}(x, y, z) = \frac{1}{2\pi} \frac{\partial}{\partial x} \int_0^\infty \left[a_i e^{u_i(z-z_{i+1})} + b_i e^{-u_i(z-z_i)} + \delta_{ij} a_p e^{-u_j|z-z_s|} \right] \times \lambda J_0(\lambda \rho) d\lambda, \quad (\text{A.1})$$

$$F_i^{TE}(x, y, z) = \frac{1}{2\pi} \frac{\partial}{\partial y} \int_0^\infty \left[c_i e^{u_i(z-z_{i+1})} + d_i e^{-u_i(z-z_i)} + \delta_{ij} f_p e^{-u_j|z-z_s|} \right] \times \lambda J_0(\lambda \rho) d\lambda, \quad (\text{A.2})$$

with

$$a_p = \begin{cases} a_p^- = \frac{m}{2\lambda^2}, \forall z < z_s \\ a_p^+ = -\frac{m}{2\lambda^2}, \forall z \geq z_s \end{cases}, \quad (\text{A.3})$$

$$f_p = f_p^- = f_p^+ = -\frac{i\omega\mu m}{2\lambda^2 u_j}, \quad (\text{A.4})$$

$$\delta_{ij} = \begin{cases} 1, \forall i = j \\ 0, \forall i \neq j \end{cases}, \quad (\text{A.5})$$

where a_i , b_i , c_i , and d_i are the potential coefficients; m is the moment of the dipole source; λ is the integral variable; z and z_s are the vertical positions of the receiver and the transmitter, respectively. The amplitudes of the direct field in TM and TE modes, which are emitted from the transmitter, are a_p and f_p , respectively. The subscript $(\cdot)_j$ represents the index of the layer containing the transmitter. The superscripts $(\cdot)^+$ and $(\cdot)^-$ denote the down-going and up-going terms, respectively.

z-oriented electric dipole source

This source has only the TM component as

$$A_i^{TM}(x, y, z) = \frac{1}{2\pi} \int_0^\infty \left[a_i e^{u_i(z-z_{i+1})} + b_i e^{-u_i(z-z_i)} + \delta_{ij} a_p e^{-u_j|z-z_s|} \right] \times \lambda J_0(\lambda \rho) d\lambda. \quad (\text{A.6})$$

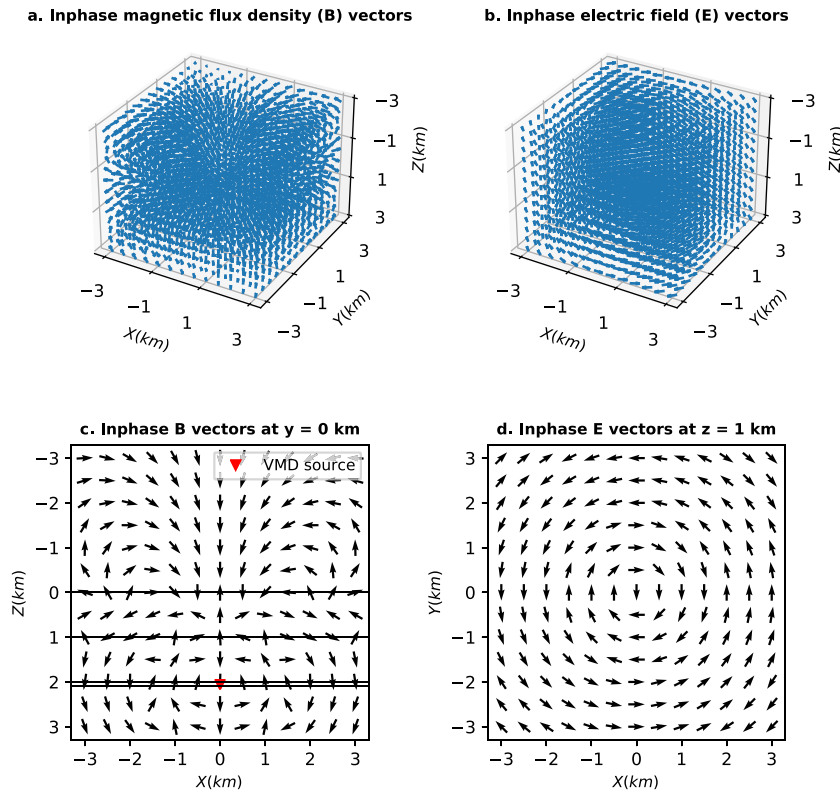


Fig. 6. The real (in-phase) component of the magnetic flux density (a) and electric field (b) in a 3D domain for a vertical magnetic dipole source located in the middle of the reservoir layer of the canonical model. (c) is a vertical section illustrating the magnetic flux density at $y = 0$ km on which the transmitter resides; (d) is a horizontal section describing the electric field on the seafloor at $z = 1$ km. (size: 120 mm \times 120 mm, 1000 dpi).

$$\text{with } a_p = a_p^- = a_p^+ = \frac{m}{2u_j}. \quad (\text{A.7})$$

$$\text{with } f_p = f_p^- = f_p^+ = \frac{i\omega\mu m}{2u_j}. \quad (\text{A.13})$$

x-oriented magnetic dipole source

The integral equations for TM and TE vector potentials can be rewritten as

$$A_i^{TM}(x, y, z) = \frac{1}{2\pi} \frac{\partial}{\partial y} \int_0^\infty \left[a_i e^{u_i(z-z_{i+1})} + b_i e^{-u_i(z-z_i)} + \delta_{ij} a_p e^{-u_j|z-z_s|} \right] \times \lambda J_0(\lambda\rho) d\lambda, \quad (\text{A.8})$$

$$F_i^{TE}(x, y, z) = \frac{1}{2\pi} \frac{\partial}{\partial x} \int_0^\infty \left[c_i e^{u_i(z-z_{i+1})} + d_i e^{-u_i(z-z_i)} + \delta_{ij} f_p e^{-u_j|z-z_s|} \right] \times \lambda J_0(\lambda\rho) d\lambda, \quad (\text{A.9})$$

where

$$a_p = a_p^- = a_p^+ = \frac{i\omega\mu\sigma_j m}{2\lambda^2 u_j}, \quad (\text{A.10})$$

$$f_p = \begin{cases} f_p^- = \frac{i\omega\mu m}{2\lambda^2} : z < z_s \\ f_p^+ = -\frac{i\omega\mu m}{2\lambda^2} : z \geq z_s \end{cases}. \quad (\text{A.11})$$

z-oriented magnetic dipole source

This source has only the TE component as

$$F_i^{TE}(x, y, z) = \frac{1}{2\pi} \int_0^\infty \left[c_i e^{u_i(z-z_{i+1})} + d_i e^{-u_i(z-z_i)} + \delta_{ij} f_p e^{-u_j|z-z_s|} \right] \times \lambda J_0(\lambda\rho) d\lambda. \quad (\text{A.12})$$

Computation of potential coefficients

In the transmitter layer, the formulae of the potential coefficients are given as

$$\left\{ \begin{array}{l} a_j = \left[a_p^+ e^{-u_j|z_{j+1}-z_s|} + R_j^{TM-} a_p^- e^{-u_j|z_j-z_s|} e^{-u_j h_j} \right] \frac{R_j^{TM+}}{1 - R_j^{TM-} R_j^{TM+} e^{-2u_j h_j}}, \\ b_j = \left[a_p^- e^{-u_j|z_j-z_s|} + R_j^{TM+} a_p^+ e^{-u_j|z_{j+1}-z_s|} e^{-u_j h_j} \right] \frac{R_j^{TM-}}{1 - R_j^{TM-} R_j^{TM+} e^{-2u_j h_j}}, \\ c_j = \left[f_p^+ e^{-u_j|z_{j+1}-z_s|} + R_j^{TE-} f_p^- e^{-u_j|z_j-z_s|} e^{-u_j h_j} \right] \frac{R_j^{TE+}}{1 - R_j^{TE-} R_j^{TE+} e^{-2u_j h_j}}, \\ d_j = \left[f_p^- e^{-u_j|z_j-z_s|} + R_j^{TE+} f_p^+ e^{-u_j|z_{j+1}-z_s|} e^{-u_j h_j} \right] \frac{R_j^{TE-}}{1 - R_j^{TE-} R_j^{TE+} e^{-2u_j h_j}}, \end{array} \right. \quad (\text{A.14})$$

where R_j^{TM+} and R_j^{TE+} are the reflection coefficients at the base in TM and TE modes, respectively, and R_j^{TM-} and R_j^{TE-} are those at the top.

If the receiver is not located in the same layer as the transmitter, the vector potentials are recursively computed by the formulae

$$\begin{cases} a_i = \frac{a_{i+1}e^{-u_{i+1}h_{i+1}} + b_{i+1} + \delta_{i+1,j}a_p^- e^{-u_j|z_j-z_s|}}{1 + R_i^{TM-} e^{-u_i h_i}}, \\ c_i = \frac{c_{i+1}e^{-u_{i+1}h_{i+1}} + d_{i+1} + \delta_{i+1,j}f_p^- e^{-u_j|z_j-z_s|}}{1 + R_i^{TE-} e^{-u_i h_i}}, \\ b_i = R_i^{TM-} .a_i, \\ d_i = R_i^{TE-} .c_i, \end{cases} \quad (\text{A.15})$$

when the receiver layer is above the source layer ($i < j$), and

$$\begin{cases} b_i = \frac{a_{i-1} + b_{i-1}e^{-u_{i-1}h_{i-1}} + \delta_{i-1,j}a_p^+ e^{-u_j|z_{j+1}-z_s|}}{1 + R_i^{TM+} e^{-u_i h_i}}, \\ d_i = \frac{c_{i-1} + d_{i-1}e^{-u_{i-1}h_{i-1}} + \delta_{i-1,j}f_p^+ e^{-u_j|z_{j+1}-z_s|}}{1 + R_i^{TE+} e^{-u_i h_i}}, \\ a_i = R_i^{TM+} .b_i, \\ c_i = R_i^{TE+} .d_i, \end{cases} \quad (\text{A.16})$$

when the receiver layer is above the source layer ($i > j$). Here, R_i^{TM-} and R_i^{TE-} are the reflection coefficients on the top of the i th layer, whereas R_i^{TM+} and R_i^{TE+} on the base of the i th layer. These coefficients are computed with an assumption that there is no reflection at the uppermost and lowermost boundaries, i.e.,

$$R_0^{TM-} = R_0^{TE-} = 0, \quad (\text{A.17})$$

$$R_{N-1}^{TM+} = R_{N-1}^{TE+} = 0. \quad (\text{A.18})$$

The recursive formulae to derive the other reflection coefficients inside the model are

$$R_i^{TM\pm} = \frac{r_i^{TM\pm} + R_{i\pm 1}^{TM\pm} e^{-u_{i\pm 1}h_{i\pm 1}}}{1 + r_i^{TM\pm} .R_{i\pm 1}^{TM\pm} .e^{-u_{i\pm 1}h_{i\pm 1}}} e^{u_i h_i (\delta_{ij} - 1)}, \quad (\text{A.19})$$

$$R_i^{TE\pm} = \frac{r_i^{TE\pm} + R_{i\pm 1}^{TE\pm} e^{-u_{i\pm 1}h_{i\pm 1}}}{1 + r_i^{TE\pm} .R_{i\pm 1}^{TE\pm} .e^{-u_{i\pm 1}h_{i\pm 1}}} e^{u_i h_i (\delta_{ij} - 1)}, \quad (\text{A.20})$$

where

$$r_i^{TM\pm} = \frac{\sigma_{i\pm 1}u_i - \sigma_i u_{i\pm 1}}{\sigma_{i\pm 1}u_i + \sigma_i u_{i\pm 1}}, \quad (\text{A.21})$$

$$r_i^{TE\pm} = \frac{u_i - u_{i\pm 1}}{u_i + u_{i\pm 1}}. \quad (\text{A.22})$$

In Eqs. (A.19) and (A.20), the exponential terms at the very end of the right-hand side are either zero or negative because of the delta function in Eq. (A.5). Thus, our formulation avoids the positive exponential everywhere in the computation procedure.

References

- [1] Constable S, Srnka LJ. An introduction to marine controlled-source electromagnetic methods for hydrocarbon exploration. *Geophysics* 2007;72(2):WA3–12. <http://dx.doi.org/10.1190/1.2432483>.
- [2] Orange A, Key K, Constable S. The feasibility of reservoir monitoring using time-lapse marine CSEM. *Geophysics* 2009;74(2):F21–9. <http://dx.doi.org/10.1190/1.3059600>.
- [3] Baranwal VC, Brønner M, Rønning JS, Elvebakk H, Dalsegg E. 3D interpretation of helicopter-borne frequency-domain electromagnetic (HEM) data from Ramså basin and adjacent areas at Andøya, Norway. *Earth Planets Space* 2020;72(1):1–14. <http://dx.doi.org/10.1186/s40623-020-01177-3>.
- [4] Andreis D, MacGregor L. Controlled-source electromagnetic sounding in shallow water: Principles and applications. *Geophysics* 2008;73(1):F21–32. <http://dx.doi.org/10.1190/1.2815721>.
- [5] Cai H, Hu X, Li J, Endo M, Xiong B. Parallelized 3D CSEM modeling using edge-based finite element with total field formulation and unstructured mesh. *Comput Geosci* 2017;99:125–34. <http://dx.doi.org/10.1016/j.cageo.2016.11.009>.
- [6] Flosadottir AH, Constable S. Marine controlled-source electromagnetic sounding: 1. Modeling and experimental design. *Geophys Res Solid Earth* 1996;101(B3):5507–17. <http://dx.doi.org/10.1029/95JB03739>.
- [7] Newman GA, Alumbaugh DL. Frequency-domain modeling of airborne electromagnetic responses using staggered finite differences. *Geophys Prospect* 1995;43:1021–42. <http://dx.doi.org/10.1111/j.1365-2478.1995.tb00294.x>.
- [8] Rochlitz R, Skibbe N, Günther T. CustEM: Customizable finite-element simulation of complex controlled-source electromagnetic data. *Geophysics* 2019;84(2):F17–33. <http://dx.doi.org/10.1190/geo2018-0208.1>.
- [9] Wannamaker PE, Hohmann GW, SanFilipo WA. Electromagnetic modeling of three-dimensional bodies in layered earths using integral equations. *Geophysics* 1984;49(1):60–74. <http://dx.doi.org/10.1190/1.1441562>.
- [10] Xiong Z. Electromagnetic fields of electric dipoles embedded in a stratified anisotropic earth. *Geophysics* 1989;54(12):1643–6. <http://dx.doi.org/10.1190/1.1442633>.
- [11] Liu R, Liu J, Wang J, Liu Z, Guo R. 1D electromagnetic response modeling with arbitrary source-receiver geometry based on vector potential and its implementation in MATLAB. *Geophysics* 2020;85(3):F27–38. <http://dx.doi.org/10.1190/geo2019-0224.1>.
- [12] Ward SH, Hohmann GW. Electromagnetic theory for geophysical applications. In: M.N. Nabighian, editor. *Electromagnetic methods in applied geophysics: Volume 1 theory*. SEG, 1988, p. 130–311. <http://dx.doi.org/10.1190/1.9781560802631.ch4>.
- [13] Key K. 1D inversion of multicomponent, multifrequency marine CSEM data: Methodology and synthetic studies for resolving thin resistive layers. *Geophysics* 2009;74(2):F9–20. <http://dx.doi.org/10.1190/1.3058434>.
- [14] Ghosh DP. The application of linear filter theory to the direct interpretation of geoelectrical resistivity sounding measurements. *Geophys Prospect* 1971;19(2):192–217. <http://dx.doi.org/10.1111/j.1365-2478.1971.tb00593.x>.
- [15] Kong FN. Hankel transform filters for dipole antenna radiation in a conductive medium. *Geophys Prospect* 2007;55:83–9. <http://dx.doi.org/10.1111/j.1365-2478.2006.00585.x>.
- [16] Key K. Is the fast Hankel transform faster than quadrature? *Geophysics* 2012;77(3):F21–30. <http://dx.doi.org/10.1190/geo2011-0237.1>.
- [17] Weniger EJ. Nonlinear sequence transformations for the acceleration of convergence and the summation of divergent series. *Comput Phys Rep* 1989;10(5–6):189–371. [http://dx.doi.org/10.1016/0167-7977\(89\)90011-7](http://dx.doi.org/10.1016/0167-7977(89)90011-7).
- [18] Werthmüller D. An open-source full 3D electromagnetic modeler for 1D VTI media in Python: empymod. *Geophysics* 2017;82(6):WB9–19. <http://dx.doi.org/10.1190/geo2016-0626.1>.
- [19] Hunziker J, Thorbecke J, Slob E. The electromagnetic response in a layered vertical transverse isotropic medium: A new look at an old problem. *Geophysics* 2015;80(1):F1–F18. <http://dx.doi.org/10.1190/geo2013-0411.1>.
- [20] GNU General Public License. <https://www.gnu.org/licenses/gpl-3.0.en.html> [Accessed 26 March 2022].
- [21] Bangerth W, Hartmann R, Kanschat G. Deal.II—a general-purpose object-oriented finite element library. *ACM Tran Math Softw* 2007;33(4):24. <http://dx.doi.org/10.1145/1268776.1268779>.
- [22] Mardal KA, Logg A, Wells G. Automated solution of differential equations by the finite element method. Springer; 2012. <http://dx.doi.org/10.1007/978-3-642-23099-8>.
- [23] PETSc 3.16. <http://www.mcs.anl.gov/petsc> [Accessed 26 March 2022].
- [24] Boost C++ library. <https://www.boost.org/> [Accessed 26 March 2022].
- [25] Python package index. <https://pypi.org/> [Accessed 26 March 2022].
- [26] Harris CR, Millman KJ, van der Walt SJ, et al. Array programming with NumPy. *Nature* 2020;585:357–62. <http://dx.doi.org/10.1038/s41586-020-2649-2>.
- [27] Hunter JD. Matplotlib: A 2D graphics environment. *Comput Sci Eng* 2007;9(03):90–5. <http://dx.doi.org/10.1038/s41586-020-2649-2>.
- [28] McKinney W. AQR capital management, pandas: a python data analysis library. 2022. <http://pandas.sourceforge.net> [Accessed 26 March 2022].
- [29] Constable S, Weiss CJ. Mapping thin resistors and hydrocarbons with marine EM methods: Insights from 1D modeling. *Geophysics* 2006;71(2):G43–51. <http://dx.doi.org/10.1190/1.2187748>.
- [30] Castillo-Reyes O, Puente Jdela, Cela JM. PETGEM: A parallel code for 3D CSEM forward modeling using edge finite elements. *Comput Geosci* 2018;119:123–36. <http://dx.doi.org/10.1016/j.cageo.2018.07.005>.
- [31] Hoversten GM, Newman GA, Morrison HF, Gasperikova E, Berg JI. Reservoir characterization using crosswell electromagnetic inversion: A feasibility study for the snorre field. *North Sea Geophy* 2001;66(4):1177–89. <http://dx.doi.org/10.1190/1.1487064>.
- [32] Commer M, Alumbaugh DL, Wilt M, Cihan A, Um ES, Petrusak R, et al. An adaptable technique for comparative image assessment: Application to crosswell electromagnetic survey design for fluid monitoring. *Geophysics* 2021;86(3):E239–56. <http://dx.doi.org/10.1190/geo2020-0430.1>.

- [33] Ma T, Chen P, Zhao J. Overview on vertical and directional drilling technologies for the exploration and exploitation of deep petroleum resources. *Geomech Geophys Geo-Energy Geo-Resour* 2016;2(4):365–95. <http://dx.doi.org/10.1007/s40948-016-0038-y>.
- [34] Cockett R, Kang S, Heagy LJ, Pidlisecky A, Oldenburg DW. SimPEG: An open source framework for simulation and gradient based parameter estimation in geophysical applications. *Comput Geosci* 2015;85:142–54. <http://dx.doi.org/10.1016/j.cageo.2015.09.015>.
- [35] Cagniard L. Basic theory of the magneto-telluric method of geophysical prospecting. *Geophysics* 1953;18(3):605–35. <http://dx.doi.org/10.1190/1.1437915>.
- [36] Høyer AS, Jørgensen F, Foged N, He X, Christiansen AV. Three-dimensional geological modelling of AEM resistivity data—a comparison of three methods. *J Appl Geophys* 2015;115:65–78. <http://dx.doi.org/10.1016/j.jappgeo.2015.02.005>.